NCEET 2025

1ST National Conference on Electronics, Electrical Engineering And Telecommunications, Challenges and Applications

University center Nour Bachir El bayadh

December 13-14, 2025, Elbayadh, Algeria

CERTIFICATE

This is to certify that 'Mohamed Ilyas Rahal' participated in the 1st National Conference on Electronics, Electrical Engineering and Telecommunications, Challenges and Applications, NCEET 2025, held in El bayadh from 13 to 14 December 2025.

And presented the paper, ID: 15

Title: Integrated MPPT and Power Control Strategy for DFIG-Based Wind Energy Systems Using PI and Sliding Mode Controllers.

Authors: Mohamed Ilyas Rahal, Adel Makhbouche, Mourad Naidji, Zine Eddine Meguetta, Gerardo Avala-Jaimes

Conference Chair

د. قنطري حسين

رئيس الملتقى

UNIVERSITY CENTER OF EL-BAYADH
1st National Conference on ELN ELEC- and TELECOM NCEET '25
INSTITUTE OF TECHNOLOGY

Director of the university center

مدير المركز الجامعي

أ.د. فراج الطيب

Integrated MPPT and Power Control Strategy for DFIG-Based Wind Energy Systems Using PI and Sliding Mode Controllers

Mohamed Ilyas, Rahal
Laboratory of Automation and Signals of Annaba (LASA)
Badji Mokhtar - Annaba University
12, P. O . Box , 23000 Annaba, Algeria
mohamed-ilyas.rahal@univ-annaba.dz

Adel Makhbouche
Advanced Control Laboratory, Université 8 Mai 1945, Guelma 24000, Algeria
makhbouche.adel@univ-guelma.dz

Mourad Naidji[1,2]
[1] *Department of Electrical Engineering,*
Badji Mokthar-Annaba University.
12, P. O . Box , 23000 Annaba, Algeria
and
[2] Laboratory of Electrical Engineering (LGE), University of M'Sila, P.O. Box 166 Ichebilia, M'Sila 28000, Algeria
mourad.naidji@univ-annaba.dz

Zine Eddine Meguetta
Advanced Automation Research Laboratory of Guelma
Higher Campus of the Lille
Lille, France
z.meguetta@gmail.com

Gerardo Ayala-Jaimes
Faculty of Sciences of Engineering and Technology, Autonomous
University of Baja California
Tijuana, Mexico
ayala.gerardo@uabc.edu.mx

Abstract— ***In order to guarantee effective Maximum Power Point Tracking (MPPT), this research proposes an integrated control strategy for a Wind Energy Conversion System (WECS). A drive train carries the mechanical energy that the wind turbine has captured to a Doubly-Fed Induction Generator (DFIG), which transforms it into electrical power. Two control systems are used to maximise this conversion: the reliable Sliding Mode Controller (SMC) and the traditional Proportional-Integral (PI) controller. To optimise power extraction, the main goal is to modify the rotor speed in response to changing wind conditions. To depict the DFIG's behaviour under various operating circumstances, a comprehensive dynamic model is created. This model serves as the basis for a power control strategy that aims to independently regulate active and reactive power, which is crucial for grid stability. To assess both controllers' performance in the entire turbine–generator system, MATLAB/Simulink is used for design and testing.***

Keywords— ***Maximum Power Point Tracking (MPPT), Doubly-Fed Induction Generator (DFIG), Proportional-Integral (PI), Sliding Mode Controller (SMC), Wind Energy Conversion System (WECS).***

I. Introduction

Renewable energy sources have been used since antiquity; ancient civilizations used sailing boats, windmills, and water wheels among other technologies. Particularly in rural areas, these systems were instrumental in driving economic development [1]. World energy consumption is driven by rising demand—mostly from coal, natural gas, and oil. Especially for air pollution and global warming produced by greenhouse gas emissions, the restricted availability and environmental concerns associated with these non-renewable sources raise big questions. The scarcity of these non-renewable resources as well as their related environmental problems raise serious doubts especially about air pollution and global warming caused by greenhouse gas emissions[2]. Considering these problems, renewable energy sources are getting growing interest as wind power is among the most workable solutions [3]. Since the first wind turbine systems (WTS) were erected in the 1980s, when their capabilities were only a few tens of kilowatts, tremendous technical development has taken place. Along with being built more regularly, wind turbines are becoming bigger and more powerful [4]. Most installed wind turbines utilize doubly-fed induction generators (DFIG) as the power conversion mechanism. This design allows efficient functioning across a broad range of wind speeds by maximizing the power extraction at every operating point. The stator is immediately connected to the grid in this whereas the rotor circuit is fed from the grid through a power converter. Because only a portion of the energy is transmitted through it [5], the converter's required capacity and cost are much cheaper than those of full-capacity converters used in variable-speed turbines with stator-side control[5]. This quality is one of the main causes dFIG-based systems frequently reach great power. Furthermore, the ability to change the connection's voltage point to the grid provides adaptability and improves general system performance [6]. To accomplish this, the present research analyzes the strong control of a wind energy conversion system (WECS) of the Doubly-Fed Induction Generator (DFIG) type so as to improve its total efficiency. Typical control techniques have two main disadvantages, according to the literature: inadequate damping [7] and poor dynamic response. As a result, there has been an increase in interest in sophisticated control techniques to overcome these constraints. Prior research has examined ways to improve dynamic performance, such as sliding mode control in systems that use Permanent Magnet Synchronous Generators (PMSG) [10], backstepping control [8], and fuzzy logic control (FLC) [9]. To ensure efficient Maximum Power Point Tracking (MPPT), this paper studies the electrical and mechanical aspects of the electrical energy conversion chain, we propose a mechanical speed control strategy for a Wind Energy Conversion System (WECS) using a Doubly-Fed Induction Generator (DFIG). The wind turbine transfers mechanical

energy to the DFIG via a drive train, converting it into electrical power. Two control approaches are implemented: a robust Sliding Mode Controller (SMC) and a conventional Proportional-Integral (PI) controller. The objective is to adapt the rotor speed optimally to variable wind conditions for maximum energy extraction. A detailed dynamic model of the DFIG is developed to enable independent control of active and reactive power—critical for grid integration. The system, including both control strategies, is modeled and simulated in MATLAB/Simulink to compare their performance.

II. WIND ENERGY CONVERSION SYSTEM

A Wind Energy Conversion System (WECS) converts wind's kinetic energy into electrical energy using a wind turbine, mechanical drivetrain, and electrical generator. Its efficiency largely depends on the drivetrain's mechanical characteristics and its ability to handle wind-induced oscillations with minimal losses. Energy conversion begins with aerodynamic interaction between wind and blades, transmitting mechanical energy to the generator. WECS designs can be direct drive or include multi-stage gearboxes [11]. Accurate modeling requires a multidisciplinary approach, combining fluid dynamics, structural mechanics, and electromechanical conversion [12]. Understanding mechanical dynamics is key to enhancing efficiency, minimizing wear, and ensuring system reliability [13,14].

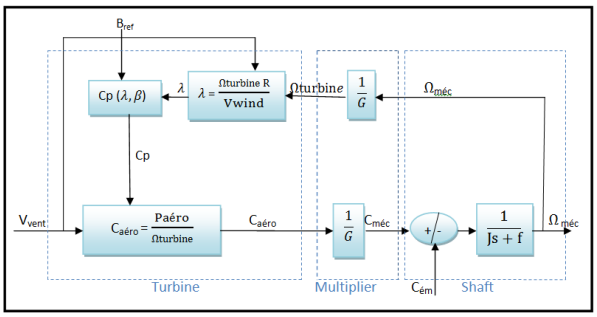

Fig. 1. Block diagram of the wind energy converter model

A. The technique of Maximum Power Point Tracking (MPPT)

Mechanical speed closed-loop control

It consists of discovering the speed of the turbine that allows for maximum power to be produced.

Two controllers are used (Proportional-Integral PI and Sliding Mode SM), whose purpose is to make the actual mechanical speed move towards the reference one, which is wind speed based.

$$C_{ém\_ref} = REG\ (\Omega_{méc\text{-}ref} - \Omega_{méc}) \qquad (10)$$

With: REG is the speed controller and $\Omega_{méc\_ref}$: is the reference mechanical speed

This reference mechanical speed depends on the turbine speed to be set ($\Omega_{turbine\text{-}ref}$) in order to maximize the extracted power. Taking into account the gearbox gain, we have:

$$\Omega_{méc\_ref} = G.\ (\Omega_{turbine\text{-}ref}) \qquad (11)$$

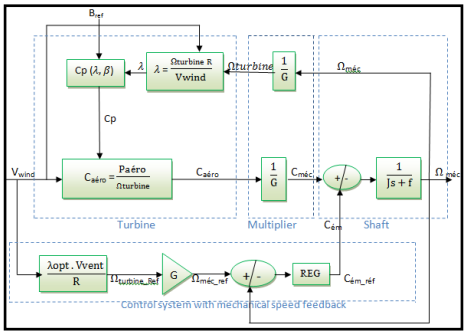

Fig. 2. Block diagram of power maximization with mechanical speed feedback control.

Wind Energy Conversion

It is clear that power is directly related to the rotor's swept area, but more crucially, to the cube of wind speed.

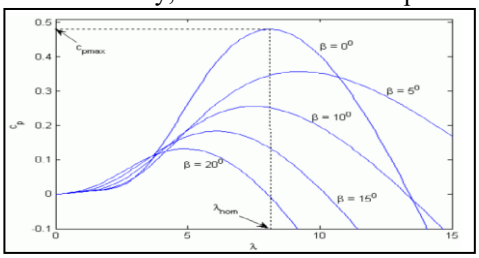

Fig. 3. Power coefficient Cp as a function of λ and β.

B. Simulation results and discussion

PI controller

Fig.4. depicts a portion of our closed-loop system controlled by a PI controller with a transfer function of the kind (Kp + Ki/s).

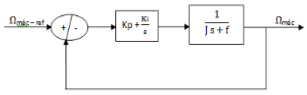

Fig. 4. The system is managed using a PI controller

Sliding Mode Controller (SMC)

The dynamic equation of the shaft is given by:

$$J\ \frac{d\Omega méc}{dt} = \sum \text{of the torques} = C_{méc} - C_{ém} - f\,\Omega_{méc}$$

$\Omega_{méc}$: is the mechanical speed of the shaft which is our output in this case.

Based on the turbine model's block diagram, the following state-space representation is defined:

$$\begin{cases} \dot{x} = -\frac{f}{J}x - \frac{1}{J}u + \frac{1}{J}P(x) \\ y = x \end{cases}$$

with :

$x = \Omega_{méc}$: the state of the system, which is the mechanical speed;

$u = C_{ém}$: the control input is the electromagnetic torque;

$P(x) = C_{méc}$: disturbance term representing the mechanical torque, considered constant.

The convergence function is defined by the Lyapunov equation; it makes the surface attractive and invariant.

$$\dot{V}(x) \le 0 \quad \Rightarrow \quad S(x)\,\dot{S}(x) \le 0$$

The command is given by

$$u = P(x) - J\,\dot{x}_d - f\,x - k_0\ Signe\ (S(x))$$

Since

$$u_{éq} = P(x) - J\dot{x}_d - f\,x$$

and

$$\dot{V}(S) = -\frac{k_0}{J}\,S(x)\ \underline{signe}\ (S(x)) = -\frac{k_0}{J}\,|S(x)|$$

which is negative, therefore, the convergence condition is satisfied. The simulation outcomes indicate that the second operating region is correctly operated by the wind energy conversion system as expected by a variable-speed turbine model and its associated control strategy with Maximum Power Point Tracking (MPPT). Figure.5 illustrates the wind speed profile imparted to the turbine with an average of about 9 m/s. At this speed, the control strategy can optimize power generation by holding the power coefficient of the turbine at its optimal level

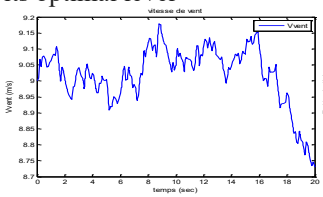

Fig. 5 .Wind speed (m/s).

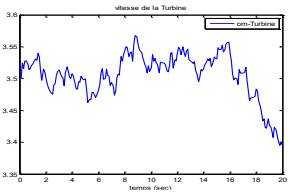

Fig. 6. Turbine speed (rad/s).

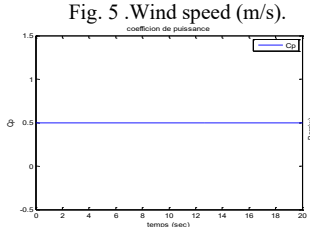

Fig. 7. Power coefficient.

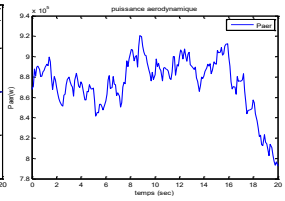

Fig.8 . Wind turbine power (W).

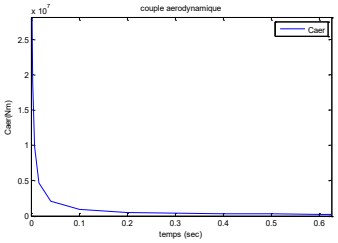

Fig. 9 .Wind turbine torque (Nm).

The control mechanism maintains the generator's mechanical rotating speed at its maximum

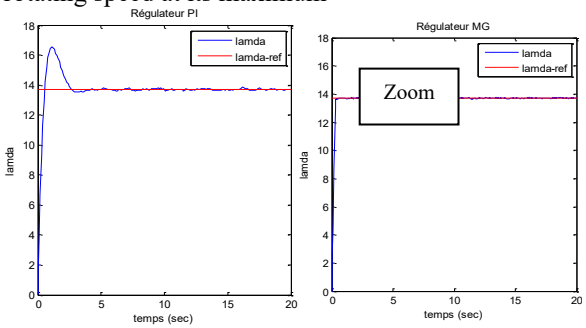

Fig. 10 . The speed ratio (λ) and its reference ((λ_{ref}) for both regulators (PI et SM).

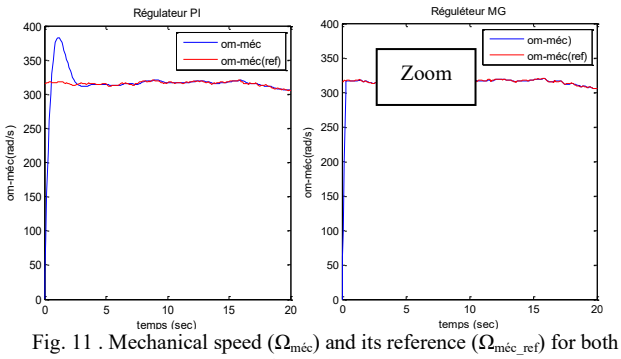

Fig. 11 . Mechanical speed ($\Omega_{méc}$) and its reference ($\Omega_{méc\_ref}$) for both regulators (PI et SM).

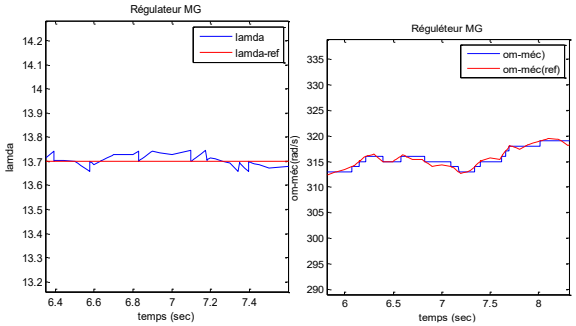

Fig. 12 . Speed ration zoom (λ) and mechanical speed ($\Omega_{méc}$) regulator (SM).

All simulations were operated under identical operating conditions to contrast the effectiveness of the two control methods, Sliding Mode Control (SMC) and Proportional-Integral (PI) (Figures 10 and 11). Mechanical speed (Figure 11) and speed ratio (Figure 10) both yield acceptable setpoint tracking. The PI controller, however, possesses significant steady-state inaccuracy and a substantial overshoot (approximately 90 rad/s). However, the SMC approach that ensures accurate monitoring of the reference signal can effectively solve these issues. SMC is also renowned for insensitivity to parameter variation and external disturbances. The Sliding Mode Control technique boasts the best overall performance in tracking accuracy and system robustness.

III. MODELING OF DOUBLY FED INDUCTION GENERATOR DFIG

The Doubly-Fed Induction Generator (DFIG) is widely adopted in wind energy systems due to its ability to efficiently operate over a broad range of wind speeds, thanks to its stator directly connected to the grid and its rotor interfaced via power converters. This partial power processing reduces converter cost compared to full-scale systems and enables voltage control at the point of interconnection, making the DFIG suitable for large-scale wind applications [16,17], [18], [19]. In [20], the DFIG is modeled using input-output representations, such as transfer functions or state-space models, to facilitate control and dynamic analysis. Park's transformation, based on [21], is employed to derive the machine's electrical equations in a simplified and structured form using the Park matrix.

$$[A] = \sqrt{\frac{2}{3}}\begin{bmatrix} \cos\psi & \cos(\psi - \frac{2\pi}{3}) & \cos(\psi + \frac{2\pi}{3}) \\ -\sin\psi & -\sin(\psi - \frac{2\pi}{3}) & -\sin(\psi + \frac{2\pi}{3}) \\ 1/\sqrt{2} & 1/\sqrt{2} & 1/\sqrt{2} \end{bmatrix} \quad (16)$$

The following relation provides the general form of the electromagnetic torque of a three-phase asynchronous machine modelled in the Park frame:

$$C_{ém} = \frac{P\,M}{Lr}(\varphi_{dr}\, i_{qs} - \varphi_{qr}\, i_{ds}) = P\,(\varphi_{ds}\, i_{qs} - \varphi_{qs}\, i_{ds}) \quad (17)$$

The following provides the stator's active and reactive powers:

$$\begin{cases} P_s = U_{ds}\, i_{ds} + U_{qs}\, i_{qs} \\ Q_s = U_{qs}\, i_{ds} - U_{ds}\, i_{qs} \end{cases} \quad (18)$$

The simulation of the 1.5 kW DFIG model provides results illustrating the behavior of key variables such as speed, torque, stator and rotor fluxes, current components, and active/reactive power. Under steady-state conditions at a constant speed of 1450 rpm, the DFIG is supplied by two ideal three-phase voltage sources: 220 V, 50 Hz at the stator and 12 V at the rotor, both operating at the same frequency.

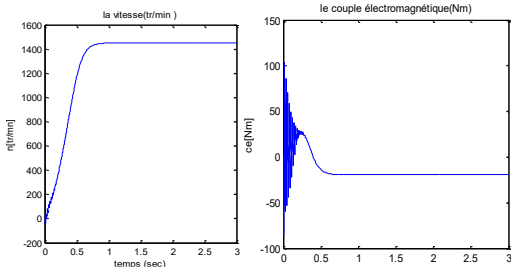

Fig. 13. Electromagnetic speed and torque.

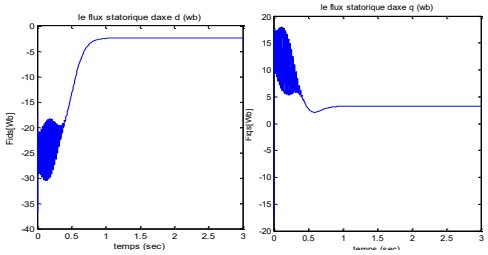

Fig. 14. The components of the stator flux of axis dq.

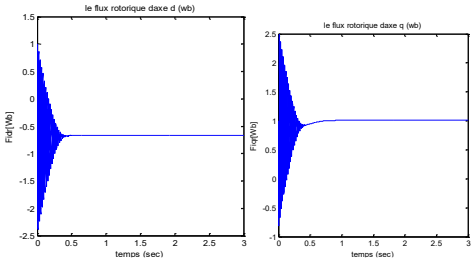

Fig. 15. The components of the rotor flux of axis dq.

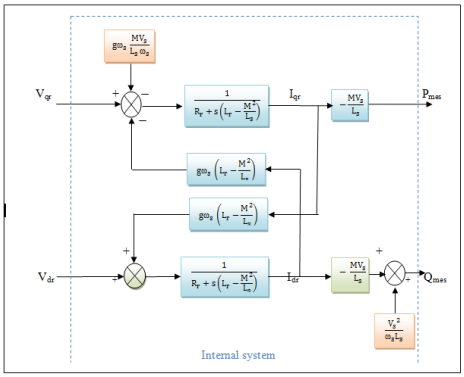

Fig. 16. Block diagram of the system to be regulated.

In this section, we present the regulation of the active and reactive powers of the machine using the remarks made in the previous paragraph. The link between, on the one hand, the active power and the voltage, and on the other hand, the reactive power and the voltage, has been highlighted.
In this study, two regulators are used for PI and MG power control.
PI: Proportional-Integral regulator;
MG: Sliding-Mode regulator.

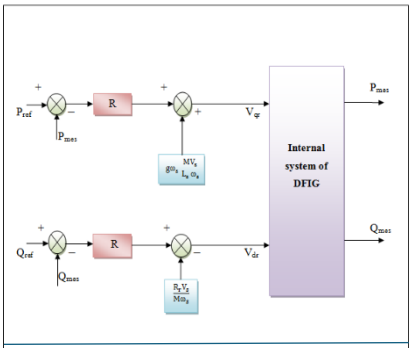

Fig. 17. Block diagram of the direct control

A. *Control of Doubly-Fed Induction Generator by PI*

Speed and simplicity are the strengths of the PI controller, which is why it is used in MADA control, with integral action improving steady-state performance and proportional action improving transient performance.

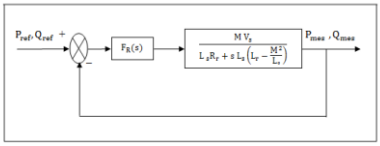

Fig. 18. PI regulated system..

$$\begin{cases} FTBF = \dfrac{FTBO}{1+FTBO} = \dfrac{K_p \dfrac{M\,V_S}{L_S\,(L_r - \frac{M^2}{L_S})}}{s + K_p \dfrac{M\,V_S}{L_S\,(L_r - \frac{M^2}{L_S})}} \\ FTBF = \dfrac{1}{1 + s.\tau_r} \qquad \text{with : } \tau_r = \dfrac{1}{K_p} \cdot \dfrac{L_S\,(L_r - \frac{M^2}{L_S})}{MV_S} \end{cases}$$

with : τ_r : is the real time constant of the system, and will be chosen during the simulation in order to offer the best compromise between performances, especially since an unsuitable value would cause disturbances during transient regimes and would cause unwanted overshoots and instabilities [19].

$$\begin{cases} K_p = \dfrac{1}{\tau_r} \cdot \dfrac{L_S\,(L_r - \frac{M^2}{L_S})}{M\,V_S} \\ K_i = \dfrac{1}{\tau_r} \cdot \dfrac{R_r\,L_S}{M\,V_S} \end{cases} \quad (24)$$

B. *Control of the DFIG using Sliding Mode Control(SMC):*

We extract the derivatives of the rotor currents we obtain the following state model:

$$\begin{cases} \dot{x} = \begin{bmatrix} \dot{x}_1 \\ \dot{x}_2 \end{bmatrix} = \begin{bmatrix} -\frac{R_r}{L_r\sigma} & 0 \\ 0 & -\frac{R_r}{L_r\sigma} \end{bmatrix} \begin{bmatrix} x_1 \\ x_2 \end{bmatrix} + \begin{bmatrix} -\frac{MV_S}{L_S L_r \sigma} & 0 \\ 0 & -\frac{MV_S}{L_S L_r \sigma} \end{bmatrix} \begin{bmatrix} u_1 \\ u_2 \end{bmatrix} + \begin{bmatrix} 1 & 0 \\ 0 & 1 \end{bmatrix} \begin{bmatrix} P_1 \\ P_2 \end{bmatrix} \\ y = \begin{bmatrix} 1 & 0 \\ 0 & 1 \end{bmatrix} \begin{bmatrix} x_1 \\ x_2 \end{bmatrix} \end{cases}$$

C. Control law computation:

Let us recall the command algorithm which is:

$$u = u_{éq} + u_n$$

For the first control law u_1 *and the second control law* u_2 :

$$u_1 = \frac{L_s L_r \sigma}{M V_s}\left(P_1 - \dot{x}_{1d} - \frac{R_r}{L_r \sigma} x_1\right) - k_1 \text{signe}\,(S_1(x))$$

$$u_2 = \frac{L_s L_r \sigma}{M V_s}\left(P_2 - \dot{x}_{2d} - \frac{R_r}{L_r \sigma} x_2\right) - k_2 \text{signe}\,(S_2(x))$$

The following figure shows the block diagram of direct control by a sliding mode (MG) type regulator:

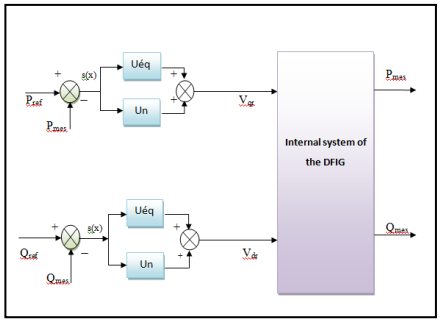

Fig. 19 . Block diagram of direct control by the MG regulator.

Two Controllers will be tested for setpoint tracking
This test involves performing active and reactive power increments while maintaining a constant DFIG drive speed.

D. Simulations results:

Setpoint tracking

Test Conditions

Driven machine at 1450 tr/min

- AT t = 2s : active power step (Pref goes from 2000W to -2000W)
- AT t = 2.5s : reactive power step (Q_{ref} goes from 1000VAR to -1000VAR)

The simulation results (cf.Figures 20) present the different active and reactive power setpoint tracking curves obtained for direct control. It can be seen that the power steps are well tracked by the generator, for both active and reactive power. There are notable distinctions between the two controllers (PI and Sliding Mode) when compared. Although there are still minor oscillations, the Sliding Mode Controller responds quickly and has zero steady-state error and no overshoot. The PI controller, on the other hand, has axis coupling that results in notable transient oscillations, overshoot during setpoint changes, and considerable delay. Additionally, when active and reactive powers drop, disruptions show themselves. In contrast to the PI controller, the sliding mode control exhibits a more noticeable chattering effect.

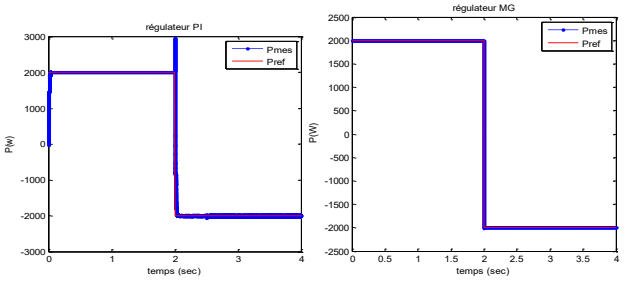

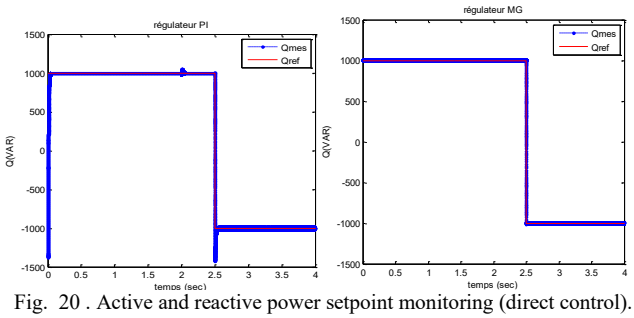

Fig. 20 . Active and reactive power setpoint monitoring (direct control)..

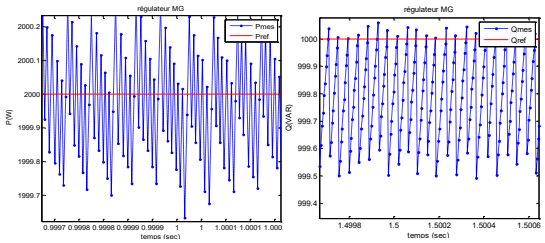

Fig. 21 . Zoom of active and reactive power (direct control) MG regulator.

In practice, the term discontinuousu $= -$ k signe (S) with $k > 0$ .This can cause unmodeled high-frequency dynamics, resulting in "reluctance" or "chattering" (characterized by strong oscillations around the surface). To reduce or eliminate chattering, three types of controls are used:

• Composite control based on Utkin's equivalent vector principle;
- Higher-order sliding modes;
- Boundary layer solution (modified sign function).

Test of Robustness

The robustness test consists of testing the stability of the DFIG model in the face of parameter variations, to verify that the control remains compliant with the constraints. This is essential because in a real system, these parameters can vary due to physical phenomena and inaccuracies in identification. Simulations will be performed by modifying the resistances and inductances independently to identify the variables where the controls are not robust.

Test conditions: Resistances increased by 50% and inductances reduced by 20%, with a constant speed of 1450 tr/m.

Test: At t = 2s: Pref goes from 2000W to -2000W.
At t = 2.5s: Qref changes from 1000 VAR to -1000 VAR.
Inductances decrease by 20%.

Results and interpretations

Figure 22 shows the evolution of power during a 20% variation in inductances Ls, Lr, and Msr. It has been observed that direct control becomes unstable with a PI controller, particularly at t = 2.5s, when the active power (Q) changes from 1000 VAR to -1000 VAR, causing an increase in oscillations around the reference (Figure 22). In addition, the change in the reactive power Q setpoint with the PI controller causes an overshoot of 500 VAR.

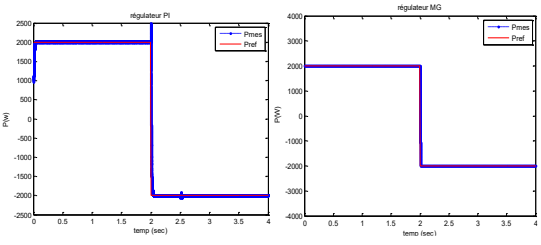

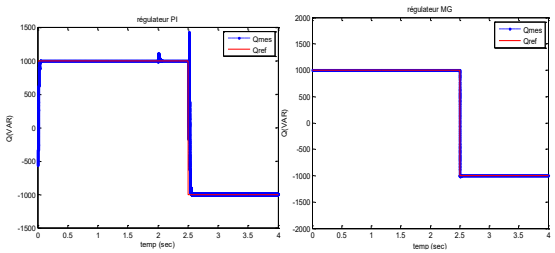

Figure 22 : Robustness test with 20% reduction in inductance(direct control).

IV. Conclusion

This paper explores a control strategy for Maximum Power Point Tracking (MPPT) in wind energy systems utilizing a Doubly-Fed Induction Generator (DFIG). It compares two controllers: Proportional-Integral (PI) and Sliding Mode Controller (SMC). The results from simulations indicate that the SMC outperforms the PI controller in setpoint tracking, thus improving the performance and reliability of modern wind power systems. The second section of the paper focuses on modeling and controlling a DFIG using both PI and SMC techniques to regulate active and reactive power independently. Simulation findings show that while both controllers offer similar performance in setpoint tracking, the SMC demonstrates faster response, reduced steady-state error, and better robustness. Despite some chattering issues, the SMC is regarded as a more reliable and easily implementable solution for wind energy systems. The paper concludes by suggesting the consideration of practical implementation in future work.

References

[1] J. M. Adànez, B. M. Al-Hadithi, and A. Jiménez, "Wind turbine multivariable optimal control based on incremental state model," *Asian J. Control*, vol. 20, pp. 1–13, 2018.
[2] N. T. A. Tuyet and S. Y. Chou, "Maintenance strategy selection for improving cost-effectiveness of offshore wind systems," *Energy Convers. Manage.*, vol. 157, pp. 86–95, 2018.
[3] A. A. Chhipa, V. Kumar, S. Vyas, and R. R. Joshi, "MPPT optimisation techniques and power electronics for renewable energy systems," *Int. J. Swarm Intell.*, vol. 1, 2021.
[4] M. A. Akbari, J. Aghaei, and M. Barani, "Convex probabilistic allocation of wind generation in smart distribution networks," *IET Renew. Power Gener.*, vol. 11, no. 9, pp. 1211–1218, 2017.
[5] N. Jargalsaikhan, H. Masrur, A. Iqbal, S. Rangarajan, S. Byambaa, and T. Senjyu, "A control algorithm to increase the efficient operation of wind energy conversion systems under extreme wind conditions," *Int. Energy Rep.*, vol. 8, pp. 11429–11439, 2022.
[6] V. Kumar, A. S. Pandey, and S. K. Sinha, "Grid integration and power quality issues of wind and solar energy systems: a review," in *Proc. Int. Conf. Emerg. Trends Electr., Electron. Sustain. Energy Syst. (ICETEESES)*, IEEE, pp. 1–6, Mar. 2016.
[7] M. Rajendran and L. A. Kumar, "Modeling and simulation of a DFIG-based wind energy system," in *Lecture Notes Electr. Eng.*, vol. 687, Springer, Singapore, pp. 31–49, 2020.
[8] H. Itouchene, F. Amrane, and Z. Boudries, "Robust control of DFIG wind turbines in sub/super-synchronous operation using integral backstepping controller," *J. Renew. Energies*, pp. 23–31, 2023.
[9] A. Z. Mohamed, M. N. Eskander, and F. A. Ghali, "Fuzzy logic control based maximum power tracking of a wind energy system," *Renew. Energy*, vol. 23, pp. 235–245, 2001.
[10] S. H. Lee, Y. J. Joo, J. Back, and J. H. Seo, "Sliding mode controller for torque and pitch control of wind power system based on PMSG," in *Proc. Int. Conf. Control, Autom. Syst. (ICCAS)*, pp. 1079–1084, 2010.
[11] T. Ackermann and L. Söder, "An overview of wind energy – status 2002," *Renew. Sustain. Energy Rev.*, vol. 6, no. 1–2, pp. 67–127, 2002. [Online]. Available: https://doi.org/10.1016/S1364-0321(02)00005-6
[12] S. Heier, *Grid Integration of Wind Energy: Onshore and Offshore Conversion Systems*, Wiley, 2014.
[13] E. Hau, *Wind Turbines: Fundamentals, Technologies, Application, Economics*, Springer, 2013.
[14] I. Griche, S. Messalti, K. Saoudi, M. Y. Touafek, and F. Zitouni, "A new controller for voltage and stability improvement of multi-machine power system tuned by wind turbine," Math. Model. Eng. Problems, vol. 8, no. 1, pp. 27–35, 2021.
[15] A. Fernández-Guillamón, E. Gómez-Lázaro, E. Muljadi, and Á. Molina-García, "Power systems with high renewable energy sources: A review of inertia and frequency control strategies over time," Renew. Sustain. Energy Rev., vol. 115, p. 109369, 2019.
[16] M. L. Chen, H. Zhang, and L. Xie, "Optimization of energy storage systems for hybrid renewable energy applications: A review," *Energy Convers. Manage.*, vol. 230, p. 113841, 2021.
[17] J. Kim, S. Lee, and S. Park, "Advanced control strategies for power electronics systems," *J. Power Electron.*, vol. 38, pp. 109-118, 2023.
[18] M. R. Patel, "Recent advancements in power electronic switching techniques," *IEEE Trans. Power Electron.*, vol. 39, pp. 542-552, 2022.
[19] L. Zhang, Z. Liu, and M. Y. Zhan, "Control strategies for doubly fed induction generators in wind energy systems," *Renew. Energy*, vol. 145, pp. 1258–1269, 2023.
[20] N. Wang, L. Li, and X. Liu, "Modelling and control of electrical machines for sustainable energy applications," *Energy Reports*, vol. 28, pp. 359–372, 2023.
[21] E. M. Pérez, L. M. García, and F. R. Jiménez, "Optimization of electric traction systems with energy-efficient control strategies," *IEEE Trans. Ind. Appl.*, vol. 59, pp. 2893–2904, 2023.

APPENDIX 1

Parameters of the wind turbine used:

Average wind speed: $V_{moy} = 9$ m/s.
Wedge angle: B = 2.
Number of blades: P = 3.
Radius of the rotor: R = 35.25 m.
Time constant value: $\tau = 4$ s.
Air density: $\rho = 1.22$ Kg/m^3.
Gearbox gain (gear ratio): G = 90.
Moment of inertia: J = 1000 Kg.m².
Viscous friction coefficient: f = 0.0024 N.m.s/rd.

Regulator Parameters

Mechanical Speed Control (Turbine Part):

PI Controller	Sliding Mode Controller (SMC)
Kp = 2.800 10^3	
Ki = 4000	$K_o = 1\ 10^6$

APPENDIX 2

Parameters used for simulations.
Nominal values:
Mechanical power: Pm = 1.5 KW.
Nominal speed: Nn = 1450 tr/min.
Nominal stator frequency: $f_{sn} = 50$ Hz.
Nominal rotor frequency: $f_{rn} = 50$ Hz.
Nominal stator single voltage: $V_{sn} = 220$ V.
Nominal rotor single voltage: $V_{rn} = 12$V.
Nominal stator line current: $I_{sn} = 4.3$ A.
Nominal rotor line current: $I_{rn} = 1.5$ A.

Parameters of DFIG:
Stator winding resistance: $R_s = 1.75\ \Omega$
Rotor winding resistance: $R_r = 1.68\ \Omega$.
Stator cyclic inductance: $L_s = 295$ mH.
Rotor cyclic inductance: $L_r = 104$ mH.
Mutual cyclic inductance: $M_{sr} = 165$mH.
The number of pole pairs: p = 2.

Mechanical constants of the DFIG :
Moment of inertia: $J_{méc} = 0.01$ Kg.m².
Viscous friction coefficient: f = 0.0027 N.m.s/rd.

PI regulator	MG regulator
Kp = 0.0410	$K_1 = 80$
Ki = 5.8753	$K_2 = 70$

Mechanical constants of the DFIG :
Moment of inertia: $J_{méc} = 0.01$ Kg.m².
Viscous friction coefficient: f = 0.0027 N.m.s/rd.

PI regulator	MG regulator
Kp = 0.0410	$K_1 = 80$
Ki = 5.8753	$K_2 = 70$

1st National Conference on Electronics, Electrical Engineering and Telecommunications, Challenges and Applications

The first NCEET-2025

Held in University centre Nour Bachir El bayadh
Sunday 14th December, 2025

Time	Sunday/December 14,2025
8h00 – 8h30	Welcome & Registration
8h30 – 9h15	Opening Ceremony Allocation of Pr Faradj Tayeb Rector of University center Nour Bachir El bayadh Allocation of Dr GUENTRI Hocine Chair NCEET conference
9h15 – 10h15	Keynote Dr Benyahia Kadda Cybersecurity for IA: A core requirement, not an option
10h 30 – 13h 00	Oral session /02 Parallel Rooms
14h00 – 15h00	Poster session
18h00 – 20h00	Online session/03 Parallel Rooms

Importantnote: **The registration process will be available during the days of the seminar**

08h00 – 8h30	Welcome & Registration
8h30 – 9h15	Opening Ceremony Allocation of Pr Faradj Tayeb Rector of University center Nour Bachir El bayadh Allocation of Dr GUENTRI Hocine Chair NCEET conference

Plenary Session:

Chairs: …Dr GUENTRI Hocine….& …Dr Djouhri Moustapha……

9h15 – 10h15	Keynote Dr Benyahia Kadda Cybersecurity for IA: A core requirement, not an option

10h30 - 13h00	Oral session / 02 Parallel Rooms

Room1: Central Library

Chairs : Pr.Hamid A …&…Pr Alaoui Tayeb…..&… Dr Reguig S K

Oral session 1: Electrical engineering				
Time	**ID**	**Title**	**Authors**	**Affiliation**
10h30-10h45	**Paper_ID_7**	Comparative analysis of the effects of hybrid renewable energy integration	medjdoubi khadidja	University center of El bayadh
10h 45 – 11h 00	**Paper_ID_17**	Assessment of Optimal PV Placement in IEEE 9-Bus System using powerworld simulator	smail Latifa	University center of El bayadh
11h 00 – 11h 15	**Paper_ID_34**	Control and optimization of a hybrid PV-wind system under variable climatic conditions for isolated loads	Cheggoufi Nourel Houda	University center of El bayadh
11h 15 – 11h 30	**Paper_ID_52**	Fuzzy logic-based mppt command and p&o method applied to a photovoltaic system	Guetti Youcef islem	University center of El bayadh
11h 30 – 11h 45	**paper_ID_68**	Improved Maximum Power Point Tracking Algorithm Using Fuzzy Logic for Wind Conversion System	Behloul Rabia	Universty of Djelfa
11h45 – 12h 00	**paper_ID_77**	Fuel cell-battery hybrid powered light electric vehicle (scooter)	Saied Boumediene	University of Bechar
12h00 – 12h 15	**paper_ID_79**	Enhanced Transformer Fault Diagnosis Using Ensemble Machine Learning and Square Root–Normalized Dissolved Gas Analysis Data	Boudjella Fatima Zohra	University of Ain temouchent
12h15 – 12h 30	**paper_ID_74**	Modeling and Simulation of a Scalable Solar-Powered Green Hydrogen Production System in the Ouargla Region, Algeria	Abdelatif Gadoum	University of Ouargla
12h30 – 12h45	**paper_ID_86**	Advanced simulation and modeling design of the solar water lift system in an innovative way	Khouani Houssam Eddine	University center of El bayadh

Room2: AMPHI C

Chairs: Pr Belkheir Mohamed …. &…. Dr Ziani Djamila

Oral session 1: Electronic and TELECOM				
Time	**ID**	**Title**	**Authors**	**Affiliation**
10h 30 – 10h 45	**paper_ID_87**	Adaptive Lightweight Defense Against Version Number Attacks: Stability and Energy Impact Evaluation in RPL	BOUKHOBZA Mohamed Achref	University center of Elbayadh
10h 45 – 11h 00	**paper_ID_55**	Design of a Single-Axis Solar Tracker Prototype Based on a Zelio Programmable Logic Controller (PLC)	BENALI Abdelkrim	University of El bayadh
11h 00 – 11h 15	**paper_ID_25**	Bio-Inspired Optimization Algorithms for Renewable Energy Systems: A Review and Application Perspectives	taha bachir ammour	University of Adrar
11h 15 – 11h 30	**paper_ID_39**	IsoLink-Health: A Satellite-Based Edge Computing Framework for Smart Healthcare in Isolated Environments	Fatima Zahra ZAOUI	University of Laghouat
11h30- 11h45	**paper_ID_65**	Study and Evaluation of the Performance of Channel Coding and Decoding Functions in a Multipath Environment: A State of the Art	Dahmani Rekia	University center of Elbayadh
11h 45 – 12h 00	**paper_ID_49**	The evolution of Antenna: from a device to a technology	Fateh Allah Merazga	University center of Elbayadh
12h 00 – 12h 15	**paper_ID_60**	Analytical and Exploratory Study of Photonic Crystal Fibers	Abdelkader Boutaleb	University center of Elbayadh
12h 15 – 12h 30	**paper_ID_88**	Optimizing RPL IoT Networks: Performance Evaluation of an Enhanced Route Selection Strategy	BOUKHOBZA Mohamed Achref	University center of Elbayadh
12h 30 – 12h 45	**paper_ID_31**	Effect of the Conductivity on the Underground Electric Field Radiated by Lightning return stroke on Tall Sructures:Analysis using EM models and the3D-FDTD method	Mohamed Abdelghani	University of Saida
12h 45 – 13h 00	**paper_ID_86**	Couches minces nanocomposites ZnO–SnO_2 : Optimisation structural et optique pour les applications optoélectroniques et photovoltaïques	Benali Mohamed Amine	University center of Elbayadh

14^h00 -15^h00	**Poster Session**

The hall of the Central Library

Chairs: Dr Bendjilali R I, Dr Smail l…..&..Dr Benali M A …..&..Dr Sellam A

ID	Title	Authors	Affiliation
paper_ID_1	Placement of "FACTS" devices in an electrical energy network	Aissa Belhadj	University of El bayadh
paper_ID_62	Comparative Study of Classical Perturb and Observe and Fuzzy Logic Control-Based MPPT Techniques for Photovoltaic Energy Conversion Systems	MILOUDI Khaled	University of Bechar
paper_ID_63	Enhanced MPPT Performance for Photovoltaic Systems Using Sliding Mode Control: A Comparative Study with the Perturb and Observe Method	MILOUDI Khaled	University of Bechar
paper_ID_11	Comparison between P&O, INC, and PSO MPPT techniques	Aissa Assas	University of El bayadh
paper_ID_26	Applications of Swarm Intelligence and Evolutionary Algorithms in Next-Generation Telecommunication Systems	taha bachir amour	University of Adrar
paper_ID_53	Comprehensive Analysis of a Three-Phase Grid-Connected Solar Photovoltaic System	Guetti Youcef islem	University of El bayadh

paper_ID_56	Design of a PIC16F876-Based Temperature Controller Using One Wire Digital Sensor DS18B20	BENALI Abdelkrim	University of El bayadh
paper_ID_72	Power Loss Reduction in Radial Distribution Systems via Modified Global Harmony Search Approach for Optimal DG Allocation and Sizing	Houari BOUDJELLA	University of Ouargla
paper_ID_73	Computation of Electric Fields in the Vicinity of High Voltage Power Line	Tahar ROUIBAH	University of Ouargla
paper_ID_75	DC Bus Voltage Regulation under Variable Solar Irradiance in PV Systems	Moufok Hadjer	University of Ouargla
paper_ID_76	Fuzzy logic-based speed enhancement of Electric scooter: Design and Analysis	Saied Boumediene	University of Bechar
paper_ID_78	Energy Mangement of hybrid battery/SC For Electric Scooter	Saied Boumediene	University of Bechar
paper_ID_80	Digital Contribution to the Study of Pumping a Ferromagnetic Nanofluid Using an MHD Induction Pump	Abderrahim MOKHEFI	University of Bechar
paper_ID_81	Design of a Micro Converter Powered by a Photovoltaic Panel	Mustapha Belhabib	USTO
paper_ID_82	Design of an LC microfilter and integration into a solar photovoltaic microconverter	Fatima Zohra MEDJAOUI	USTO
paper_ID_83	Assessment of the Electromagnetic Environment Around an Industrial MV/LV Transformer with Shielding Deficiency: Analysis and Corrective Measures	Djilali MAHI	University of Laghouat
paper_ID_84	Study of the electromagnetic performance of a planar coil	Fatna BAHLOULI	USTO
Paper_ID_18	Analysis of the Impact of Wind Power Integration on Power Flow and Losses in an Electrical Network	Reriballah Hafidha	University of Relizane
paper_ID_85	Experimental examination of an altered triboelectric charging system	Djouhri Mostapha	University center of El bayadh
paper_ID_71	Speed control of universal motor using MCU based firing angle control	Djillali Nasri	University of Tiaret

18h00 -20h00	**Online session**

Room1: https://meet.google.com/erv-avzf-ovp
Chairs: DR DAHBI A …..&…Dr NOUR M

Online session: Electrical engineering				
Time	**ID**	**Title**	**Authors**	**Affiliation**
18h 00–18h 10	**paper_ID6**	Enhancement of solar thermal power plants' ability to generate electricity	Mandi benaissa	University of Tlemcen
	paper_ID10	A fuzzy logic approach to detect and classify electrical fault in three-phase squirrel-cage motor	Yassine Bouhelassa	University of Oran 2
	paper_ID15	Integrated MPPT and Power Control Strategy for DFIG-Based Wind Energy Systems Using PI and Sliding Mode Controllers	Mohamed Ilyas Rahal	University of Anaba
	paper_ID19	Performance Evaluation of the Sandia Array Performance Model for Grid-Connected Photovoltaic System Using Artificial Bee Colony Optimization	Yassine BOUDOUAOUI	ESGEE Oran
	paper_ID20	Estimating parameters values of battery lead-acid using Simulink Design Optimization	DJAHFA SALIM	University of Khenchela
	paper_ID23	Comparative Analysis of Dandelion Optimizer and P&O Algorithms for MPPT in PV Systems under Standard and	Hadjer CHABANA	University of Anaba

		Partial Shading Conditions		
	paper_ID30	Innovative Control Techniques for Stand-Alone Self-Excited Induction Generators	zabouri abdelhamid	ENP Oran
	paper_ID32	Optimizing the PID Controller Using the Genetic Algorithm for Temperature Control in Household System	meroua kertous	University of Setif 1
	paper_ID35	Smart Grid Inspired PSO-MPPT Framework for Standalone DC Hybrid Microgrids	yassmine boucherit	University of Constantine1
	paper_ID37	An adaptive state of charge estimation method For Battery PV	Mourad Tiar	University of Biskra
	paper_ID6	Enhancement of solar thermal power plants' ability to generate electricity	Mandi benaissa	University of Tlemcen
	paper_ID46	Model-Based Fault Diagnosis Applied to the Wind Turbine Pitch System	chaima gherari	University of Souk Ahras
	paper_ID67	Computation of Electric Fields in the Vicinity of High Voltage Power Line	Tahar ROUIBAH	University of Ouargla
	paper_ID27	Dynamic voltage support for wind turbine system using STATCOM for grid integration	Soumia Kail	University of Bechar
	paper_ID_12	Impact of Massive Wind Penetration on the Dynamic Stability of Electrical Transmission Grids	Mourad Naidji	University of Anaba
	paper_ID_69	Maximum Power Point Tracking (MPPT) Review and Methods	Amir Eddine Bouguettoucha	University of Mila
	Paper_ID_29	Comparative Optimization of Fractional-Order PID Controllers for Precise Quadcopter Agrissive Trajectory Tracking	aissa benhammou	University of Bechar

Room 2: https://meet.google.com/eja-weyn-gei
Chairs: … Dr Djelaila S..&…Dr MERMOUH S

Online session: Electronic				
Time	**ID**	**Title**	**Authors**	**Affiliation**
18h 00–18h 10	**paper_ID_4**	Evaluating the Impact of Dopants in CdS Buffer Layers for CZTS Solar Cells	Sarra Merabet	University of Mostaganem
	paper_ID_5	Enhancing BHJ Organic Solar Cells Performance through Internal Resistance Management	Samia Moulebhar	University of Mostaganem
	paper_ID_24	Assessing EEMD versus VMD for Enhanced Diagnosis of Inner Bearing Defect	yasser damine	University of Biskra
	paper_ID_36	State estimation for discrete events systems modeled by Petri net	Fayssal Arichi	University of Constantine1
	paper_ID_42	Practical Approach to Calibration of Solar Irradiance Instruments	Oulimar IBrahim	URERMS Adrar
	paper_ID_45	Intelligent drone for autonomous fire detection using artificial vision and on-board intelligence	Oussama Slimani	USTHB
	paper_ID_48	Luenberger control of speed sensorless PMSM	MEDJMADJ Slimane	UBBA
	paper_ID_51	Enhancing IoT Security with AI-Based IDS: A Case Study on BoT-IoT Dataset	Abdelkader Hadj-Attou	University of Blida
	paper_ID_59	Mathematical based magnetic resonance imaging slice selection technique	Mehdi KHALFALLAH	University of Msila

Room 3: https://meet.google.com/czi-wdth-vko
Chairs: Pr ROUISSAT M …..&…Dr MENEZLA F

Online session: Telecommunication				
Time	**ID**	**Title**	**Authors**	**Affiliation**
18h 00–18h 10	**paper_ID_9**	Broadband PCB Bandpass Filters For Millimeter Wave Applications: SIW Circular CSRRs	Rahali bouchra	University of Tlemcen
	paper_ID_21	Predicting Link Quality in Mobile Wireless Sensor Networks: GMLA, Markov Models, and Comparative Insights	Abderrahmane TAMALI	University of Setif 1
	paper_ID_28	A 2D Photonic Crystal Biosensor for Early Cancer Detection Using GaAs Nanoring Resonator	Bachir RAHMI	INRE
	paper_ID_33	An IoT/M2M-Enabled Intelligent Remote Patient Monitoring Framework for Smart Healthcare Systems	Rania Djehaiche	University of Bordj BouAreridj
	paper_ID_64	Focusing Synthetic Aperture Radar Imagery with the Range Doppler Algorithm	Issam Tifouti	University of Skikda
	paper_ID_66	A Dual Side-by-Side Slotted Patch MIMO Antenna with Connecting Vias for mm-Wave 5G applications	Berhab Souad	ENSTTIC, Oran
	paper_ID_43	QoS-Aware Resource Allocation in 6G OFDMA Systems with RIS and Network Slicing	yacine ouazziz	University of Bejaia
	paper_ID_50	Design and Performance Analysis of a Full-Duplex millimeter wave RoF-GPON System Using dual port OFDM Modulation	abdennour fellag chebra	University of Tlemcen
	paper_ID_54	A Compact High-Efficiency Microstrip Antenna with Partial Ground Structure for Broadband Ka-Band 5G	Assia LOMBARKIA	University of Batna
	paper_ID_57	Material-Dependent Performance Optimization of a Compact Wideband 1–3 THz Vivaldi Antenna for Imaging and High-Data-Rate Links Using HDPE, Quartz, Silicon, Alumina, and TiO	khalida khodja	University of Boumerdes
	paper_ID_61	Latency-Aware and Bitrate-Efficient Evaluation of uQUIC Vs UDP in VANET Video Streaming	Hana Elhachi	University of Guelma
	paper_ID_38	Drone-Assisted Telecommunication Networks: A Comprehensive Survey of Applications, Roles, and Existing Works	Tarek Bouzid	University of Laghouat
	paper_ID_3	Experimental Evaluation of DigiMesh Protocols for Optimized Wireless Sensor Network (WSN) Performance	Halima sahraoui	University of Saida
	paper_ID_22	Loop Closures in LiDAR Graph-SLAM for Improved Accuracy	Istighfar Chettih	University of Laghouat